# Morpholinium-Modified, Polyketone-Based Anion Exchange Membranes for Water Electrolysis

Simone Bonizzoni, Diego Stucchi, Tommaso Caielli, Eva Sediva, Michele Mauri, and Piercarlo Mustarelli*[a]

Water electrolysis is by far the most appealing method to produce green hydrogen. Among the possible technologies, Anion Exchange Membrane (AEM) water electrolyzers are promising in the medium term, as they make it possible to avoid critical and noble materials as catalyst components. However, AEMs are still lacking in performance and stability, which has become the current research focus. Here, we report the facile and inexpensive chemical modification of polyketone (PK) with a functional unit encompassing morpholinium as the positively charged group, and the fabrication of self-standing membranes. The synthesis products are investigated with an ensemble of physico-chemical and spectroscopic techniques, including solid-state and time-domain NMR, FT-IR, and thermal analysis. The membranes show good Ion Exchange Capacity values in the range 1.48–2.24 mmol g$^{-1}$. A preliminary electrolysis test shows that the PK-based membrane has performance comparable to that of a commercial one.

## Introduction

Hydrogen plays a key role in the EU's roadmap to carbon neutrality.[1] In fact, it is estimated that hydrogen could supply up to 20% of the energy demand.[2] This transition will require further performance and cost improvements in the crucial technologies of water electrolyzers (WEs) and fuel cells (FCs).[3–5] State-of-the-art proton exchange membrane fuel cells (PEMFCs) and electrolyzers (PEMWEs) use perfluorinated ionomers (PFI), which allow high conductivity while also granting the desired chemical and electrochemical stability in operational conditions.[6–9] Nonetheless, they have some significant drawbacks, including the need for platinum group metals (PGMs) as catalysts that result in their large capital costs, and a high fuel crossover with respect to other systems, like those based on polybenzimidazoles.[10] This later issue occurs both when molecular hydrogen and methanol are used in FCs.[11] The first drawback is chiefly caused by the acidic working conditions.[12] To solve this problem, anion exchange membranes (AEMs)[13] are gaining attention since their working environment is highly alkaline near the electrodes. This causes the electrochemical reaction mechanisms to be different from those occurring in acidic conditions.[14] As a result, the electrochemical process can be promoted without the need of PGM catalysts, which greatly reduces the cost.[15–17]

AEMs are usually made of polyelectrolytes obtained from a wide range of polymers, including polystyrene, unsaturated polypropylene and polyethylene, polybenzimidazoles, poly-(vinylbenzyl chloride) and poly(arylene ethers).[8] The charged active group is often based on nitrogen atoms, either in the form of quaternary ammonium (QA) sites, or embedded in heterocycles like imidazolium, benzimidazolium and pyridinium. Alternative active sites, not based on nitrogen, include phosphonium and sulphonium cations, or metal-based systems where multiple charges are present on each side chain.[13,18,19] Even the best AEMs still suffer of several drawbacks, including low chemical stability in the presence of hydroxide anions, and low conductivity values. The first problem causes a non-ideal durability.[20–22] Regarding the second issue, it is caused by the much lower mobility of OH$^-$ when compared to H$^+$ of the commercial PFI-based PEMs.[13,23] Consequently, much higher ion exchange capacity (IEC) values are needed in AEMs when compared to PEMs. This, however, causes a decrease in mechanical properties of the membranes because of the excessive swelling of the polymers.[20] One last point of concerns is the carbonation process, that occurs when the membranes are exposed to CO$_2$, which meaningfully decreases the conductivity of the polymer and thus the performance of the device.[13,22] Potential solutions to these shortcomings come in the form of the development of appropriately phase-segregated polymers,[24] cross-linking procedures,[25] and hybrid membranes.[26] In particular, the first approach aims at the creation of a hydrophobic backbone that provides the desired mechanical properties, with an inter-dispersed hydrophilic phase (caused by the charged groups in the lateral chains) that provides the ionic conductivity.[24] Cross-linking could similarly improve the mechanical properties of the final polymer and reduce the crossover.[25] Lastly, the use of inorganic nanofillers dispersed in the organic membranes could improve the

[a] Dr. S. Bonizzoni, D. Stucchi, T. Caielli, Dr. E. Sediva, Prof. Dr. M. Mauri, Prof. Dr. P. Mustarelli
Department of Materials Science
University of Milano Bicocca
Via Cozzi 55, 20125 Milano (Italy)
E-mail: piercarlo.mustarelli@unimib.it

polymer durability.[26] Alternatively, the use of cycloaliphatic rings as active sites, where the quaternary ammonium is embedded in, could increase the stability of the membrane.[27]

Recently, a few groups[28,29] investigated the use of poly-ketones as a starting material to produce AEMs, thanks to their optimal thermal, chemical, and electrochemical resistance coupled with good mechanical properties, and the ease of chemical modification and low-cost production.[30] Both QA and imidazolium were investigated as active sites. In this paper we report on the chemical modification of a commercial poly-(ethylketone) with morpholinium as an active site suitable for application in WEs and FCs. The synthesis procedure is accompanied by a thorough thermal and spectroscopic characterization of the products, as well as by preliminary in-cell tests showing encouraging results.

## Results and Discussion

Infrared and NMR spectroscopies were carried out to investigate the success of the first and second reaction steps reported in Figure 1.

### FT-IR

Figure 1 reports the FT-IR spectra of the samples after Step_1 and Step_2. The main signals are due to non-reacted 1,4 diketone unit, pyrrole ring and N-propylmorpholine, which are highlighted in Figure 3 in orange, blue and green, respectively. The $-CH_2-$ stretching and bending of the PK backbone were detected at 2956, 2920 and 1356 cm$^{-1}$, while the C=O stretching of the carboxyl group was noticed at 1700 cm$^{-1}$.[29,31] The pyrrole ring generated the stretching of C=C-H at 3100 cm$^{-1}$, at 1640 and 1580 cm$^{-1}$ the stretching of C=C and at 1259 cm$^{-1}$ the bending of C-N. The $CH_2$-N stretching and bending at 2800 and 1406 cm$^{-1}$ and the C-O-C stretching at 1100 cm$^{-1}$ were correlated to the morpholine structure.[32,33] The

broad signal (*) in the 3500–3200 cm$^{-1}$ region should be correlated to O-H stretching modules of moisture due to the hydrophilic nature of morpholine.[33] After methylation, Step_2 spectrum showed the $CH_3$-N stretching at 2850 cm$^{-1}$ and the O-H stretching band at 3440 cm$^{-1}$. Both these signals confirmed the success of the reaction.[34]

### Solid state NMR

Figure 2 shows the $^{13}$C-$^1$H CPMAS spectra where the PK and pyrrole signals are highlighted in yellow and light green, respectively. The starting material generated two peaks at 207.3 and 34.7 ppm, due to carboxyl group (a) and the $-CH_2-$ of the polymer backbone (b).[35,36] The formation of pyrrole ring generated two signals at 130.3 and 103.4 ppm (e, f) and caused the shift of $-CH_2-$ peaks at 39.9 and 19.8 ppm (c, d). The propyl group, between pyrrole and morpholine rings, generated the peaks at 50.0, 27.2, 53.3 ppm (g, h, i), while the morpholine group produced the signals at 55.0 and 65.4 ppm (m, n).[33] After methylation, Step_2 spectrum showed significant changes in 70–10 ppm zone due to tetraalkyl-ammonium group presence. The (n, i, m) signals converged into a unique peak centred at 60 ppm, the h carbon moved to 22.0 ppm and the new methyl group (p) generated a shoulder of the c, b peaks at 47.2 ppm.[37–39] The signal marked with * was correlated to silicon oil impurities. The spectra of PK_0.3 and PK_0.7 showed similar results (see Figure S3).

The functionalization degree (from 0.3 to 0.7) was also qualitatively checked by $^{13}$C-$^1$H CPMAS measurements. Figure 3 reports the spectra of the three compositions after Step_1, normalized to the intensity of the pyrrole carbon at 130 ppm, which allows to observe the signals trends vs. the stoichiometry. The carboxyl (207.3 ppm, violet) and $-CH_2-$ (34.7 ppm, green) signals decreased, whereas the $-CH_2-$ pyrrole increased (39.9 ppm, orange) as expected from stoichiometry.
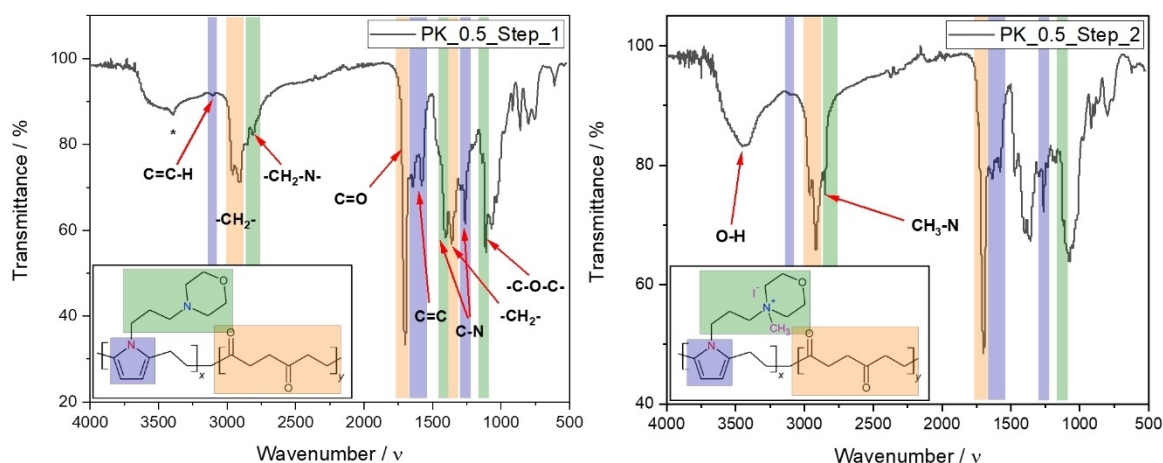


**Figure 1.** FT-IR spectra PK_0.5 after Step_1 (left) and Step_2 (right), with assignation of non-reacted 1,4 diketone unit (orange), pyrrole ring (blue) and N-propylmorpholine (green).
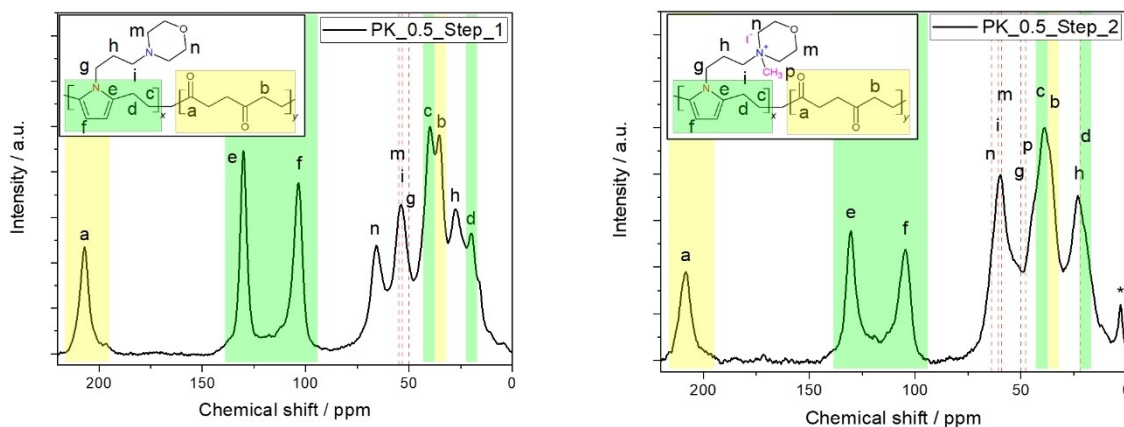
**Figure 2.** $^{13}C$-$^1H$ CPMAS NMR spectra of PK_0.5 after Step_1 (left) and Step_2 (right), with highlights of PK (yellow) and pyrrole carbons (green). The morpholine/morpholinium carbon peaks are emphasized by red dashed lines.
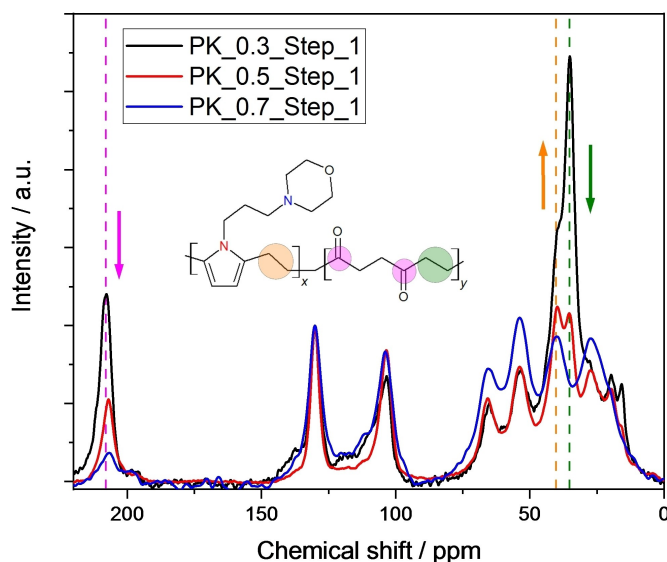


**Figure 3.** $^{13}C$-$^1H$ CPMAS spectra of samples with 0.3, 0.5 and 0.7 stoichiometry after Step_1.



**Figure 4.** TGA curves of PK, PK_0.5_Step_1 and PK_0.5_Step_2.

### Thermal analysis

Figure 4 shows the TGA behaviour of pristine PK and of sample PK_0.5 after Step_1 and Step_2. Pristine PK is stable up to ~360°C in agreement with literature.[40,41] Step_1 sample showed a ~1 wt% loss below 100°C, due to dichloromethane (DCM) and hexafluoroisopropanol (HFIP) evaporation, followed by a multi-step degradation process in the region of 150–550°C. Step_2 sample showed a greater (~4 wt%) loss below 100°C, due to solvents and absorbed water, and then followed by a larger stability region which extends well above 200°C. This greater thermal stability is due to ionic interactions introduced by nitrogen quaternization. The samples PK_0.3 and PK_0.7 showed similar behaviours (see Figure S4).

Figure 5 reports the second heating DSC scans of the three samples after Step_1 and Step_2 in the temperature region from 0 to 150°C. In this temperature range PK did not show any significant thermal feature (see Figure S5). As a matter of fact,
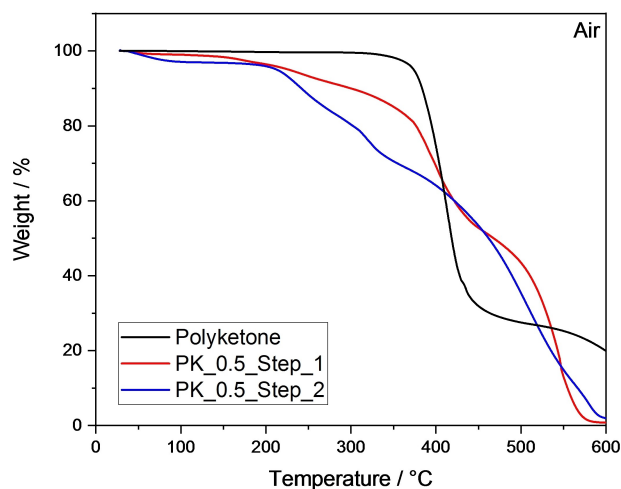
the melting temperature of PK is reported above 200°C.[40] The samples after Step_1 showed a glass transition, $T_g$, in the range of 30–60°C depending on the ratio between the pyrrole and the PK moieties. The increase of pyrrole-morpholine fraction shifts the $T_g$ to higher temperature, reflecting an increase of the matrix stiffness chiefly due to the aromatic rings. The small endotherm at ~130°C is likely due to a first order phase transition, which can be attributed to the melting of a crystalline phase, as it does not correspond to significant weight losses in the TGA (see Figure 4). This melting peak, whose intensity is roughly independent from composition, shifts to lower temperatures by increasing the functionalization degree. Similar melting processes were previously reported on pyrrole-functionalized PKs.[40]

The samples after Step_2 did not show any $T_g$ in the 30–60°C range. However, small baseline deflections could be observed in the range 90–100°C for the three samples. At the same time, the melting endotherm above 120°C increased in intensity except for sample PK_0.5 where this thermal feature was not observed. The absence of this feature can be due to the dynamic nature of the DSC experiment. However, further
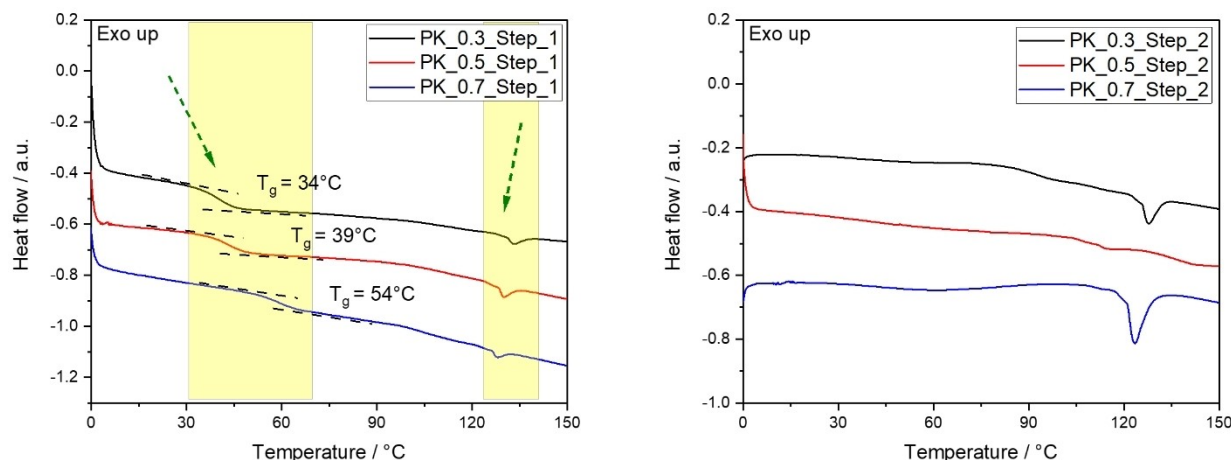
**ChemElectroChem**

Research Article
doi.org/10.1002/celc.202201077

**Chemistry Europe**
European Chemical
Societies Publishing

**Figure 5.** DSC curves of the samples PK_0.3, PK_0.5 and PK_0.7 after Step_1 (left) and Step_2 (right).

studies are needed to clarify this peculiar thermal behaviour. More information on polymer chain dynamics can be obtained by TD-NMR. Because of its anomalous thermal behaviour, as well as for being the optimal compromise for functional applications (see below), we focused our attention on the PK_0.5 sample.

**Time Domain NMR (TD-NMR)**

Figure 6 shows the FIDs acquired with the application of a MSE refocusing block. This pulse sequence is specifically developed to offset the loss of rapidly decaying signal associated to rigid phases during instrumental dead time, and thus is consistently used to quantitate rigid and mobile fractions in multiphase systems.[42] Generally, faster decays correspond to slower local motions, and more in detail dynamics and local organization dictate the functional shape of the FID: exponential for mobile phases, Gaussian for amorphous polymers under the $T_g$, etc.[43]

It can be immediately seen that PK and PK_0.5 after Step_1 and Step_2 at 40 °C are very similar, with the fast decay expected for rigid polymers: the signal goes to 0 in less than 0.2 ms. The pristine polymer displays an Abragamian decay component usually associated to crystalline systems and appearing as a small "bump" in the FID (signed with an arrow in Figure 8 left). As the temperature is increased to 140 °C, the mobility increases, and all decays become slower but the Abragamian component in PK is conserved. This indicates a polycrystalline system, where the interfacial regions display an increase in local chain mobility while the crystals are still far below the melting point (see Figure S6). The Step_2 sample is also relatively unaffected by the temperature increase: the shape remains mostly Gaussian, and the data at the highest temperature can be well-fitted as the summation of 67% Gaussian component and a 33% exponential with low spin-spin
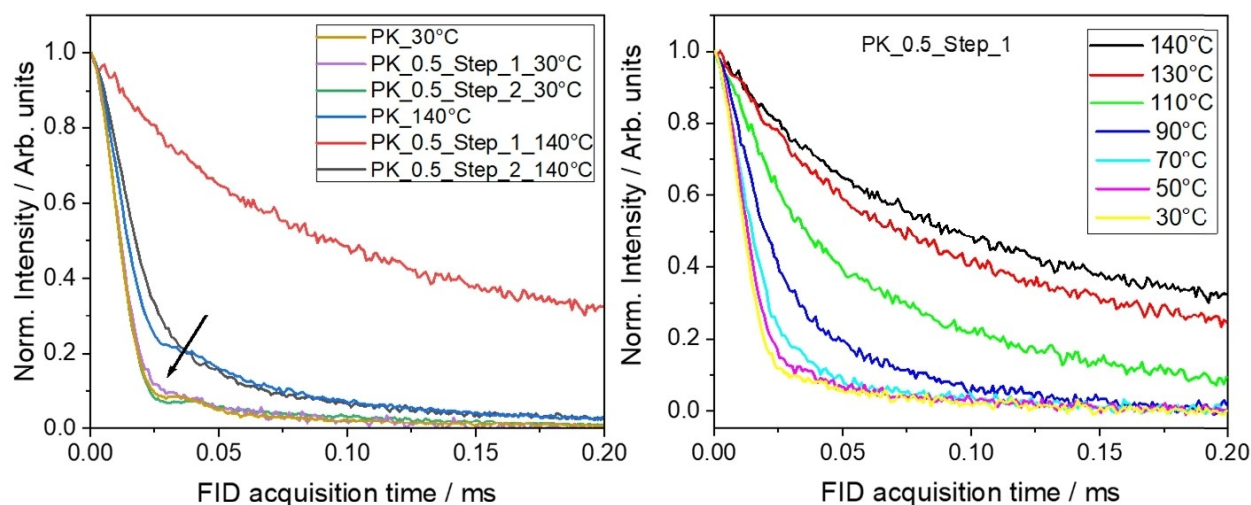


**Figure 6.** Time domain NMR: (left) the comparison of PK, PK_0.5 after Step_1 and PK_0.5 after Step_2 at 30 °C and 140 °C; (right) behavior of PK_0.5 after Step_1 vs. temperature.

**ChemElectroChem**

Research Article
doi.org/10.1002/celc.202201077

**Chemistry**
**Europe**
European Chemical
Societies Publishing

relaxation time, $T_2^*$ (see Figure S7). In contrast, the behavior of PK_0.5 after Step_1 is starkly different, with a far slower relaxation that is better understood by looking in detail at the entire temperature evolution (Figure 8, right). Up to 70 °C the FID is almost constant, while from 90 °C the relaxation evolves rapidly.

Previous studies in amorphous polymers associated this behavior to the onset of glass transition.[44] Our interpretation is that the addition of morpholine during Step_1 produces a structure that cannot crystallize anymore due to the bulkiness of the side chains, resulting in an amorphous polymer with glass transition around 40–60 °C. Further reaction (Step_2) produces an ionic system that is locally immobilized by Coulomb forces,[45] and thus presents a relevant increase of $T_g$, possibly above 100–120 °C, in good qualitative agreement with the DSC results. In the following we plan to perform a careful, and systematic study on the different stoichiometries.

**IEC and ionic conductivity measurements**

Table 1 reports the IEC experimental values for the samples with different stoichiometries compared with the corresponding theoretical values. The experimental values are 20–30 % lower than the theoretical ones depending on the stoichiometry. However, the measured values are large enough to allow acceptable electrochemical properties. The ionic conductivity at 80 °C is slightly higher than $10^{-3}$ S cm$^{-1}$, not optimal for electrolysis applications, but enough to deserve further investigations on this system.

Figure 7 reports the behavior of ionic conductivity vs. temperature for the three examined samples after anion exchange (Step_3 in Scheme 1), and the corresponding Arrhenius plot with the best-fits used to calculate the activation energies, $E_a$, for OH$^-$ motion reported in Table 1. Whereas our conductivity values are of the same order of magnitude of those reported by the group of Di Noto,[29] they are a factor of ~25 lower than those of Zhou et al.,[28] who used 1-(3-

**Table 1.** IEC, ionic conductivity, and activation energy for the three samples.

| Sample | IEC exper. [mmol g$^{-1}$] | IEC theor. [mmol g$^{-1}$] | σ [S cm$^{-1}$] at 80 °C | $E_a$ (eV) |
|---|---|---|---|---|
| PK_0.3 | 1.48 | 1.88 | $1.7\times10^{-3}$ | 0.16 |
| PK_0.5 | 1.74 | 2.61 | $2.9\times10^{-3}$ | 0.28 |
| PK_0.7 | 2.24 | 3.14 | $4.0\times10^{-3}$ | 0.28 |

aminopropyl)imidazole instead of 3-morpholinopropylamine. We replicated their synthesis by employing the same functional unit, the only difference being the employed commercial polyketone (M630A, Mw = 100,000 Hyosung Co. Ltd., Seoul, Korea, instead of our AKROTEK® PK 7336, AKRO, Germany), but we were not able to reproduce the conductivity data, even if the activation energy values were similar. We infer this difference could be due to some properties of the PK matrix, e.g.: chain length, polydispersity, additives, etc., which led to different microphase (hydrophobic vs. hydrophilic) separation. Further studies are in progress, including the use of the same PK used by Zhou et al.

For a more complete analysis, Table 2 compares the physico-chemical parameters of our membranes with those previously reported on similar polyketone-based AEMs. The behaviors of water uptake and swelling ratio vs. temperature are reported in Figure S8 for the PK_0.3, PK_0.5 and PK_0.7 membranes. All the membranes showed a small increase with temperature of both water uptake and swelling ratio.

**Electrolysis preliminary tests**

Indeed, PK_0.7 showed higher IEC and conductivity values than PK_0.5. However, from the point of view of thermal stability, the sample PK_0.5 showed better thermal properties as demonstrated by the absence of relevant thermal features (see Figure 7). Therefore, it seemed to offer the best compromise. For this reason, here we are reporting the tests on PK_0.5_
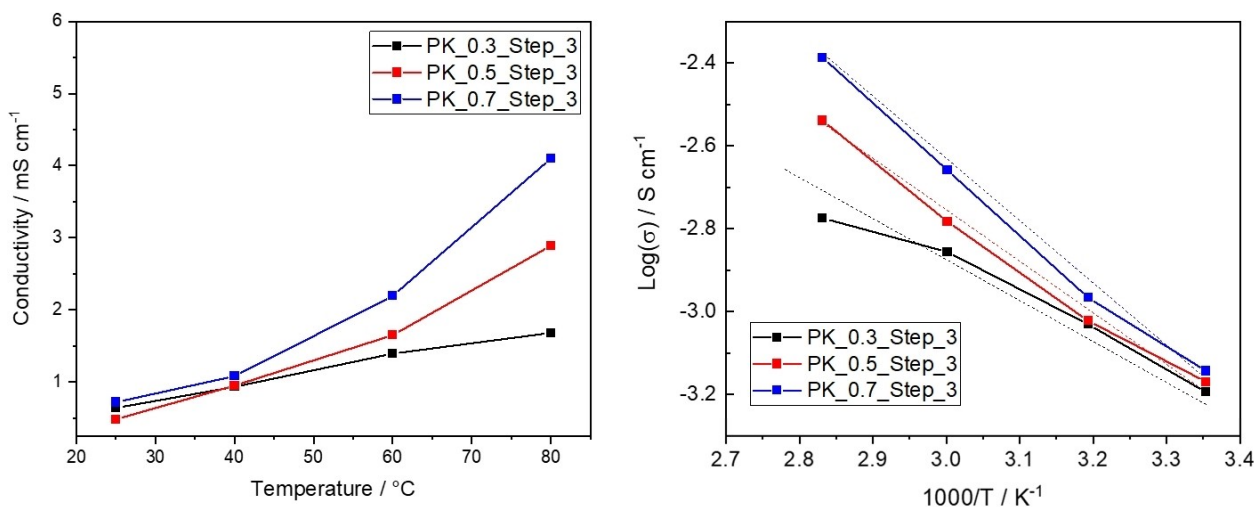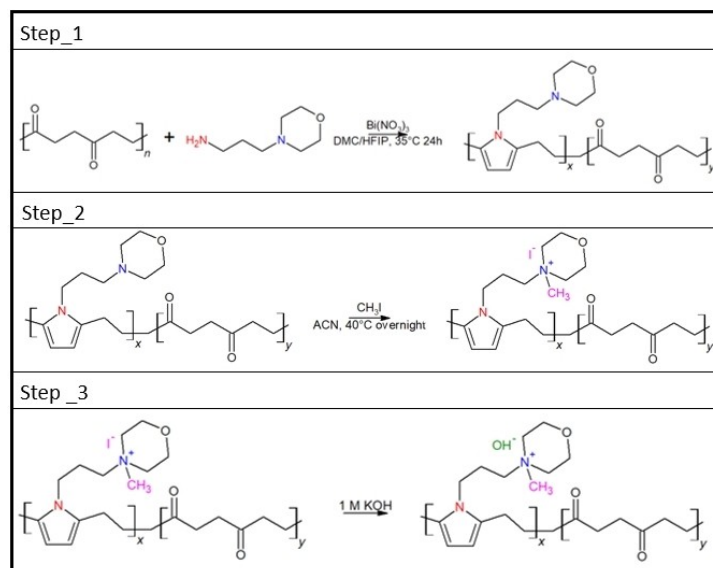


**Figure 7.** (left) ionic conductivity vs. temperature; (right) Arrhenius plot of the ionic conductivity.

**ChemElectroChem**

Research Article
doi.org/10.1002/celc.202201077

**Chemistry
Europe**
European Chemical
Societies Publishing

**Scheme 1.** Synthesis procedure.

**Table 2.** ionic conductivity, σ: a) measured through plane; b) measured in plane; c) measured by Broadband Electric Spectroscopy (BES). WU = water uptake. SR = swelling ratio. λ = hydration number. The values with the asterisk were obtained by visual graph interpolation.

| AEM | σ [mS cm$^{-1}$] | IEC [mmol g$^{-1}$] | WU [%] | SR [%] | λ | Ref. |
|---|---|---|---|---|---|---|
| PK_0.3 | 1.7 (80 °C)$^a$ | 1.48 | 23.7 (60 °C) | 7.9 (60 °C) | 8.9 | this work |
| PK_0.5 | 2.9 (80 °C)$^a$ | 1.74 | 38.2 (60 °C) | 10.5 (60 °C) | 11.5 | this work |
| PK_0.7 | 4.0 (80 °C)$^a$ | 2.24 | 51.3 (60 °C) | 18.7 (60 °C) | 13.5 | this work |
| QAFPK-1-3-AEM | 25–30* (80 °C)$^b$ | 2.71 | 15.26 (25 °C) | 13.2 (25 °C) | 2.63 | [28] |
| QAFPK-1-6-AEM | 96.8 (80 °C)$^b$ | 1.43 | 9.52 (25 °C) | 7.4 (25 °C) | 3.38 | [28] |
| QAAPIPK-1-3-C | 131.7 (80 °C)$^b$ | 2.46* | 4.4* (30 °C) | 4.9* (30 °C) | n.a. | [46] |
| QAAPIPK-1-6-C | 60–70* (80 °C)$^b$ | 1.8* | 0.88* (30 °C) | 0.8* (30 °C) | n.a. | [46] |
| PK-PDAPm | 0.9 (120 °C)$^c$ | 1.11 | 34–38 | n.a. | n.a. | [29] |
| 4MPyr-FPK | 10.5 (80 °C)$^c$ | 3.8–3.51 | 22.0 | n.a. | 3.0 | [40] |

Step_3 for potential electrolyzer applications. To rule out possible contributions from electrode manufacturing, we employed the cell reported in Figure 2 and performed the test in pure water (σ < 10$^{-6}$ S cm$^{-1}$) using two nickel foam electrodes separated with our membrane. The membrane FAA-3-50 was tested under the same conditions as the reference material. The impedance spectra with both nickel foam and stainless steel as the electrodes are reported in Figure S9.

Figure 8 shows the polarization curves. A small current was recorded below 1.2 V due to steel corrosion. H$_2$O electrolysis related currents (above 1.5 V) are small (60 mA cm$^{-2}$ at 2.5 V) when compared to state-of-the-art water electrolyzers.[4] This is imputable mainly to the experimental set-up: the measurement is indeed performed in pure water without an ionomer to increase triple phase boundaries. However, in these less-than-ideal conditions our PK based membrane attained performances comparable with those of the commercial membrane FAA-3-50. The task to investigate the durability of the membrane is not trivial, as nickel foam tends to puncture the membrane, in spite of our efforts to reduce its roughness. However, our preliminary results showed reasonable stability after 3 hours of operation, both for our membrane and for FAA-3-50. Proper durability tests would be performed with more

suited catalysts layers and will be the object of future works. For the sake of completeness, Figure S10 reports a comparison of the electrochemical performance of the three membranes developed in this study, which demonstrates that PK_0.5 works better than PK_0.3 and PK-0.7.

## Conclusion

A commercial polyketone was modified with different quantities of pyrrole-based moieties containing an aliphatic-bonded morpholinium unit. Free-standing anion exchange membranes were then fabricated, thoroughly characterized, and preliminarily tested for water electrolysis.

The AEMs showed good IEC values, whereas the ionic conductivity was not comparable to commercial AEMs and must be improved. We assume that the reason for this is connected to the microstructure of the polymer that presents a non-optimal phase separation between the hydrophobic backbone and the hydrophilic lateral chains. The cause is most likely connected to the commercial polymer we used, and we thus intend to test other commercially available polyketones to improve the final conductivity of the membranes. Regardless,
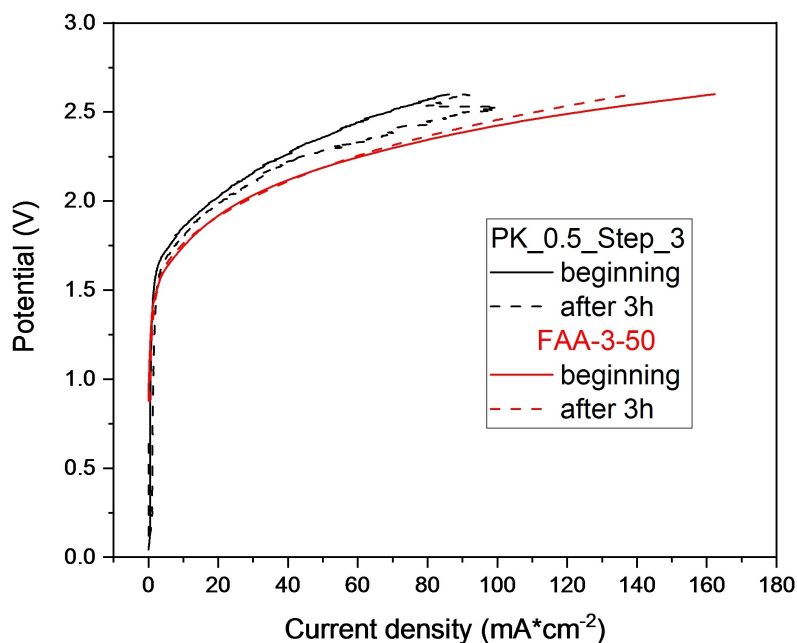
**ChemElectroChem**

Research Article
doi.org/10.1002/celc.202201077

**Chemistry Europe**
European Chemical
Societies Publishing

**Figure 8.** Comparison of the polarization curves, recorded at 80 °C, of PK_0.5 Step_3 and FAA-3-50 with nickel foam electrodes, at the beginning and after three hours of operation at 2 V.

the combined use of thermal analysis and TD-NMR allowed to shed light on the dynamics of the polymer matrix. In particular, the NMR data evidenced the presence of strong interchain ion-ion interactions, that could explain the low ionic conductivity despite the relatively high IEC value. This conclusion suggests the use of longer aliphatic pendants and/or less bulky moieties as a possible strategy to improve the ion transport properties.

The most promising membrane was also preliminary tested in an electrolysis cell, showing performances comparable to those of a commercial product.

## Experimental Section

### Raw materials

Natural high molecular weight polyketone (AKROTEK® PK 7336) (hereinafter PK) was purchased by AKRO (Germany). N-(3-aminopropyl)morpholine, iodomethane, potassium hydroxide, potassium chloride, bismuth nitrate, silver nitrate, potassium nitrate, potassium chromate, dichloromethane (DCM), hexafluoroisopropanol (HFIP), acetonitrile, HPLC-degree water were obtained by Merck. Nickel foam (Battery Cathode Substrate, 350 g m$^{-2}$) was obtained from Pi-Kem (UK). FAA-3-50 (Fumatech®) membrane was obtained from Fuel Cell Store (USA).

### Membrane fabrication

The AEM was obtained starting from pristine PK through the following steps: Paal-Knorr reaction (Step_1), methylation (Step_2), and ionic exchange (Step_3).

Step_1 (see Figure 1) is the Paal-Knorr reaction between a 1,4 – diketone unit of PK and the primary amine of N-(3-aminopropyl)-morpholine, introducing a pyrrole ring inside the polymer back-

bone. In a typical reaction, 1.5 g of PK were dissolved in 42 ml of a mixture of hexafluoroisopropanol: dichloromethane 8:12 and then 126 mg of bismuth nitrate were added as a heterogeneous catalyst as reported in the literature.[25] Then N-(3-aminopropyl)morpholine was added following stochiometric ratios of 0.3, 0.5, 0.7 between the ammine and the 1,4-diketone unit. In the following, the samples will be named PK_0.3, PK_0.5 and PK_0.7 according to their stoichiometry. The reaction was carried out at 35 °C for 24 hours under magnetic stirring. Then, to remove the catalyst, the solution was centrifuged at 9000 rpm for 5 minutes and then cast on PTFE foils using a doctor blade. The films were dried for one night at room temperature and then at 80 °C for 2 hours in air.

In Step_2, the ternary ammine of morpholine ring was converted into the corresponding tetraalkylammonium salt by alkylation with iodomethane. The reaction was performed at 40 °C overnight directly on the Step_1 membrane using a large excess of iodo-methane, and acetonitrile as a swelling agent. Then, Step_2 membranes were washed several times in acetonitrile and water and dried at room temperature.

Finally, in Step_3 the iodide-form membranes were immersed in 1 M KOH solution for 2 hours to exchange the anions, then washed several times with water and dried at room temperature. 20–60 cm$^2$ large membranes with thicknesses in the range of 40–60 μm were obtained depending on the casting parameters (see Figure S1).

### Physico-chemical and functional characterization

#### Thermal analysis

Simultaneous DSC/TGA experiments were performed by means of a TGA/DSC 1 star® system (Mettler Toledo). The TGA measurements were carried out by heating the samples up to 600 °C, with a heating rate of 10 °C min$^{-1}$ in air flux. DSC measurements were performed under N$_2$ flux with the following protocol: from 0 °C to 150 °C at 10 °C min$^{-1}$, 3 min at 150 °C, from 150 °C to 0 °C at 10 °C min$^{-1}$, 3 min at 0 °C, from 0 °C to 150 °C at 10 °C min$^{-1}$.

**ChemElectroChem**

Research Article
doi.org/10.1002/celc.202201077

**Chemistry Europe**
European Chemical
Societies Publishing

### ATR-FT-IR

The Infrared (IR) spectra were obtained on Jasco FT/IR-4100 spectrometer equipped with Attenuated Total Reflection (ATR) accessory. The spectra were recorded from 4000–500 cm$^{-1}$ with a resolution of 2.0 cm$^{-1}$. The data were analyzed with Spectra Manager™ Suite software.

### Solid-state (SS-NMR) and Time Domain NMR (TD-NMR)

The $^{13}$C-$^1$H CPMAS spectra were collected using Avance III Bruker 400 MHz spectrometer (9.4 T magnet) equipped with a 4 mm MAS probe. The $^1$H π/2 pulse was 2.5 μs, the delay time 5–200 s depending on the sample, the contact time 2.5 ms, and the signals were averaged over 1k–8k acquisitions. The MAS frequency was 10 kHz. $^{13}$C chemical shifts were referred to adamantane as a secondary standard with respect to tetramethylsilane (TMS, 0 ppm). The spectra were acquired, processed, and analysed with the software package Topspin™ 3.1 (Bruker).

Polymer chain mobility was probed by analyzing of $^1$H NMR Free Induction Decay (FID) acquired following a Magic Sandwich Echo (MSE) refocusing block. The sequence was implemented on a Minispec mq 20 ND series (Bruker), working at a Larmor frequency of 19.65 MHz. In this setup, the dead time is around 14 μs, and the 90° pulse length is 2.1 μs, for a total minimum echo time of around 110 μs. Temperature control with 0.1 K precision was provided by a nitrogen gas BVT3000 heater. These measurements were performed in the temperature range from 30 °C to 140 °C every 10 °C.

### Ion Exchange Capacity (IEC)

The Ion Exchange Capacity (IEC) of the membrane was determined by the Mohr titration method as previously reported.[47] About 100–150 mg of material were immersed in a 0.5 M KCl solution for 24 h and then washed in water by centrifugation for 4–5 times at 9000 rpm for 5 minutes, recovered, dried in vacuum at 100 °C and weighed. After that, the polymer was immersed in a 0.2 M KNO$_3$ solution for 24 h to exchange chloride counterions with nitrate. Finally, the KNO$_3$ solution was titrated with a 0.1000 M AgNO$_3$ standard solution using K$_2$CrO$_4$ as the indicator. The IEC was calculated as the ratio of the milliequivalents of membrane and its dry mass using the following Equation 1:

$$IEC \left[ \frac{mmol}{g} \right] = \frac{C_{AgNO_3} \left[ \frac{mol}{mL} \right] * V_{AgNO_3} \, [mL]}{m_{dry\,polymer} \, [g]} \qquad (1)$$

Where C(AgNO$_3$) is the concentration of AgNO$_3$ standard solution, and V(AgNO$_3$) is the final volume of titration.

### Conductivity

Through-plane conductivity of the AEM was determined with Electrochemical Impedance Spectroscopy (EIS) using SP-150 potentiostat (Biologic®), with a two-electrodes, home-made cell immersed in HPLC-degree water at controlled temperature. The cell is made of two cylindrical PTFE pieces connected by four polypropylene screws (see Figure S2). In the center of the body there are two cylindrical 316 L-stainless steel electrodes and a spring as compressor system. The electrode diameter is 0.9 cm that means an area of about 0.64 cm$^2$. Before the measurements the membranes were activated in 1 M KOH solution (Step_3) for 2 hours and then washed in distilled water several times. The measurements were carried out by soaking the cell in pure water at 20, 40, 60 and 80 °C, and EIS

was performed in the frequency range between 100 Hz and 300 kHz, with a signal amplitude of 10 mV.

### Water management

Various aspects of the membrane's water management capabilities were investigated on the Step_2 polymers. Water uptake, WU, was measured drying small pieces of membrane at 80 °C in vacuum to accurately remove any adsorbed or absorbed atmospheric water. Then they were weighed (m_dry) and subsequently immersed in 20 mL of water in a vial. The vials were kept at a given temperature with the help of either water baths (20 °C, 40 °C) or ovens (60 °C, 80 °C) for 24 h. Once this time elapsed the pieces were removed from the water and rapidly dried on a piece of paper before an accurate weighing (m_wet). The WU value was obtained from the following Equation 2:

$$WU \; (\%) = \frac{m\_dry(mg) - m\_wet(mg)}{m\_wet} * 100 \qquad (2)$$

Swelling ratios, SR, were obtained with a similar procedure (see Equation 3) using pieces of membranes in elongated form and measuring their length with a micrometer both after drying (l_dry), and after a 24 h soaking in water at different temperatures (20 °C, 40 °C, 60 °C and 80 °C).

$$SR \; (\%) = \frac{l\_dry(mm) - l\_wet(mm)}{l\_wet \; (mm)} * 100 \qquad (3)$$

Finally, the hydration number (λ) was calculated starting from the IEC and WU values as per Equation 4:

$$\lambda = \frac{w.u. \; * \; 10}{MW_{H_2O} \; * \; IEC} \qquad (4)$$

### Preliminary cell tests

The functional properties of the membrane under electrolysis conditions were preliminarily checked with a SP-150 potentiostat Biologic® on a two-electrodes cell equipped with nickel foam layers facing stainless steel electrodes, immersed in HPLC-degree water at a controlled temperature of 80 °C. The set-up is sketched in Figure 9. The measurement protocol consisted in a chronoamperometry (CA), applying 10 mA for 3 minutes, linear sweep voltammetry (LSV), from 0 to 2.5 V with scan rate of 100 mV s$^{-1}$, and EIS from 100 Hz to 300 kHz with 10 mV amplitude.
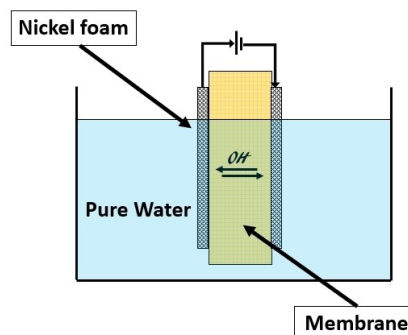


**Figure 9.** Scheme of electrolysis set-up

**ChemElectroChem**

Research Article
doi.org/10.1002/celc.202201077

**Chemistry Europe**
European Chemical
Societies Publishing

[1] EU Commission, *Delivering the Green Deal: the Role of Clean Gases including Hydrogen*, December 15, 2021, https://ec.europa.eu/commission/presscorner/detail/en/fs_21_6690

[2] M. Ierides, R. Del Valle, D. Fernandez, L. Bax, P. Jacques, F. Stassin, M. Meeus, *EMIRI Technology Roadmap: Key R&I Priorities* 2019.

[3] The Future of Hydrogen Seizing Today's Opportunities, International Energy Agency, IEA Publications 2019, 203.

[4] C. Santoro, A. Lavacchi, P. Mustarelli, V. Di Noto, L. Elbaz, D. R. Dekel, F. Jaouen, *ChemSusChem* 2022, *15*, e202200027.

[5] H. A. Miller, *Curr. Opin. Electrochem.* 2022, *36*, 101122.

[6] M. Breitwieser, M. Klingele, S. Vierrath, R. Zengerle, S. Thiele, *Adv. Energy Mater.* 2018, *8*, DOI:10.1002/aenm.201701257.

[7] V. Di Noto, T. A. Zawodzinski, A. M. Herring, G. A. Giffin, E. Negro, S. Lavina, *Int. J. Hydrogen Energy* 2012, *37*, 6120–6131.

[8] A. Z. Weber, M. M. Mench, J. P. Meyers, P. N. Ross, J. T. Gostick, Q. Liu, *J. Appl. Electrochem.* 2011, *41*, 1137–1164.

[9] C. Spiegel, *Designing and Building Fuel Cells*, Mc Graw Hill, 2007, chapter 11, pag. 192

[10] Q. Li, J. O. Jensen, R. F. Savinell, N. J. Bjerrum, *Progress in Polymer Science*, Oxford, 2009, *34*, 449–477.

[11] A. Carollo, E. Quartarone, C. Tomasi, P. Mustarelli, F. Belotti, A. Magistris, F. Maestroni, M. Parachini, L. Garlaschelli, P. P. Righetti, *J. Power Sources* 2006, *160*, 175–180.

[12] X. Z. Yuan, H. Li, S. Zhang, J. Martin, H. Wang, *J. Power Sources* 2011, *196*, 9107–9116.

[13] J. R. Varcoe, P. Atanassov, D. R. Dekel, A. M. Herring, M. A. Hickner, P. A. Kohl, A. R. Kucernak, W. E. Mustain, K. Nijmeijer, K. Scott, T. Xu, L. Zhuang, *Energy Environ. Sci.* 2014, *7*, 3135–3191.

[14] N. Ramaswamy, S. Mukerjee, *J. Phys. Chem. C* 2011, *115*, 18015–18026.

[15] S. Gottesfeld, D. R. Dekel, M. Page, C. Bae, Y. Yan, P. Zelenay, Y. S. Kim, *J. Power Sources* 2018, *375*, 170–184.

[16] M. Mandal, *ChemElectroCem.* 2020, *7(21)*, 4303–4305.

[17] H. Wu, C. Feng, L. Zhang, J. Zhang, D. P. Wilkinson *Electrochemical Energy Reviews* 2021, *4*, 437–507.

[18] K. Vezzu, A. M. Maes, F. Bertasi, A. Motz, H. Tsai, E. B. Coughlin, A. M. Herring, V. Di Noto, *J. Am. Chem. Soc.* 2018, *140(4)*, 1372–1384.

[19] D. Henkensmeier, M. Najibah, C. Harms, J. Žitka, J. Hnát, K. Bouzek, *Journal of Electrochemical Energy Conversion and Storage* 2021, *18*, 024001.

[20] Y. J. Wang, J. Qiao, R. Baker, J. Zhang, *Chem. Soc. Rev.* 2013, *42*, 5768–5787.

[21] J. B. Edson, C. S. Macomber, B. S. Pivovar, J. M. Boncella, *J. Membr. Sci.* 2012, *399–400*, 49–59.

[22] A. Zhegur-Khais, F. Kubannek, U. Krewer, D. R. Dekel, *J. Membr. Sci.* 2020, *612*, 118461.

[23] D. Marx, A. Chandra, M. E. Tuckerman, *Chem. Rev.* 2010, *110*, 2174–2216.

[24] N. Li, M. D. Guiver, *Macromolecules* 2014, *47*, 2175–2198.

[25] S. D. Poynton, J. P. Kizewski, R. C. T. Slade, J. R. Varcoe, *Solid State Ionics* 2010, *181*, 219–222.

[26] M. T. Perez-Prior, T. Garcia-Garcia, A. Varez, B. Levenfeld, *J. Mater. Sci.* 2015, *50*, 5893–5903.

[27] J. Xue, J. Zhang, X. Liu, T. Huang, H. Jiang, Y. Yin, Y. Qin, M. D. Guiver, *Electrochemical Energy Reviews* 2022, *2*, 348–400.

[28] Y. C. Zhou, Z. M. Zhang, L. Zhou, R. Y. Bao, Z. Y. Liu, M. B. Yang, W. Yang, *J. Mater. Chem. A* 2021, *9*, 14827–14840.

[29] N. Ataollahi, K. Vezzù, G. Nawn, G. Pace, G. Cavinato, F. Girardi, P. Scardi, V. Di Noto, R. Di Maggio, *Electrochim. Acta* 2017, *226*, 148–157.

[30] K. Nozaki, S. Ito, K. Matyjaszewski, M. Möller, *Alkene/CO Copolymerization, In Polymer Science: A Comprehensive Reference*, Eds., Elsevier, Amsterdam, 2012, *3*, 825–842.

[31] N. Ataollahi, F. Girardi, E. Cappelletto, K. Vezzù, V. Di Noto, P. Scardi, E. Callone, R. Di Maggio, *J. Appl. Polym. Sci.* 2017, *134*, 1–8.

[32] Merck, IR-spectrum table, on-line. www.sigmaaldrich.com/technical documents.

[33] Spectral Database for Organic Compounds SDBS, https://sdbs.db.aist.go.jp/sdbs/cgi-bin/cre_index.cgi.

[34] M. A. Shaikh, M. Farooqui, S. Abed, *Iranian Journal of Catalysis* 2018, *8*, 73–80.

[35] A. Sommazzi, F. Garbassi, *Progress in Polymer Science (Oxford)* 1997, *22*, 1547–1605.

[36] O. M. Chukanova, Y. M. Shul'Ga, G. P. Belov, *Polymer Science-Series B* 2009, *51*, 283–290.

[37] J. Aires-de-Sousa, M. C. Hemmer, J. Gasteiger, *Anal. Chem.* 2002, *74*, 80–90.

[38] D. Banfi, L. Patiny, *Chimia* 2008, *62*, 280–281.

[39] A. M. Castillo, L. Patiny, J. Wist, *J. Magn. Reson.* 2011, *209*, 123–130.

[40] G. Nawn, K. Vezzù, G. Cavinato, G. Pace, F. Bertasi, E. Pagot, E. Negro, V. Di Noto, *Adv. Funct. Mater.* 2018, *28*, 1–10.

[41] A. R. Alvi, K. Vezzù, G. Pagot, P. Sgarbossa, G. Pace, V. Di Noto, *Macromol. Chem. Phys.* 2022, *223*, 1–13.

[42] A. Maus, C. Hertlein, K. Saalwächter, *Macromol. Chem. Phys.* 2006, *207*, 1150–1158.

[43] D. Besghini, M. Mauri, R. Simonutti, *Applied Sciences (Switzerland)* 2019, *9*, 1801.

[44] S. Bonetti, M. Farina, M. Mauri, K. Koynov, H. J. Butt, M. Kappl, R. Simonutti, *Macromol. Rapid Commun.* 2016, *37*, 584–589.

[45] A. Eisenberg, *Macromolecules* 1971, *4*, 125–128.

[46] Y. Zhou, L. Zhou, C. Feng, X. Wu, R. Bao, Z. Liu, M. Yang, W. Yang, *J. Colloid Interface Sci.* 2019, *556*, 420–431.

[47] S. Bonizzoni, P. Stilli, F. Lohmann-Richters, C. Oldani, C. Ferrara, A. Papagni, L. Beverina, P. Mustarelli, *ChemElectroChem* 2021, *8*, 2231–2237.

# RESEARCH ARTICLE

**Anion exchange membranes**: Self-standing anion-conducting membranes are obtained by means of a facile and inexpensive chemical modification of polyketone (PK) with a functional unit encompassing morpholinium as the positively charged group.
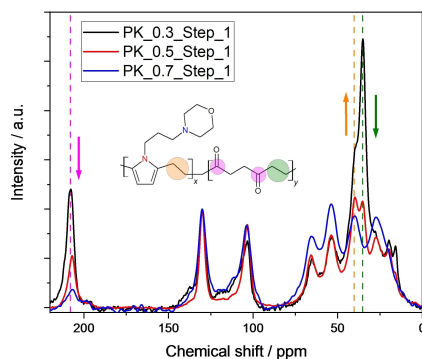
*Dr. S. Bonizzoni, D. Stucchi, T. Caielli, Dr. E. Sediva, Prof. Dr. M. Mauri, Prof. Dr. P. Mustarelli\**

1 – 10

**Morpholinium-Modified, Polyketone-Based Anion Exchange Membranes for Water Electrolysis**